

# Thermodynamic work of adhesion measurements of polymer bonded explosive constituents via the Wilhelmy plate technique and their application to AFM pull-off experiments

D M Williamson<sup>1\*</sup>, N R Hamilton<sup>1</sup>, S J P Palmer<sup>1</sup>, A P Jardine<sup>1</sup> and C Leppard<sup>2</sup>

<sup>1</sup>Cavendish Laboratory, University of Cambridge, Cambridge CB3 0HE UK

<sup>2</sup>AWE, Aldermaston, Reading, RG7 4PR

\*E-mail: dmw28@cam.ac.uk

**Abstract.** A major strength limiting factor for polymer bonded explosives above their glass-transition conditions is the magnitude of adhesion that exists between the polymeric matrix binder-system and the filler particles. Experimental measurements of the components of the free surface energy of the binder KEL-F800 have been made using the Wilhelmy Plate technique. These data can be combined with equivalent data on the filler particles to calculate the so-called Thermodynamic Work of Adhesion. This under-pinning quantity can be used to predict the levels of load (stress) required to cause debonding in different geometries. A simple geometry of interest is a spherical-cap of polymer debonding from a flat substrate. Experiments using this geometry have been performed with an Atomic Force Microscope pull-off technique to measure the critical loads (stresses) required for debonding. There is excellent agreement between the predicted values based on the Wilhelmy Plate data and the measured values from the Atomic Force Microscope. Experimental data and understanding are required for the development and validation of microstructural models of mechanical behaviour.

## 1. Introduction

Understanding of the nature of the adhesive bond between an energetic crystal and its binder system is a key consideration when trying to model the global failure behaviour of polymer bonded explosives (PBXs) [1-4]. The intrinsic energy required to break the bond between an adherend and an adhesive is referred to as the thermodynamic work of adhesion (TWA). The TWA can be estimated from knowledge of the surface properties of the adherend and the adhesive if we assume the latter wets the former. What is required of each is the surface energy,  $\gamma$ , which is the sum of the polar and the dispersive components,  $\gamma_p$  and  $\gamma_d$  respectively. The TWA is simply the sum of the two surface energies less a correction due to the interfacial solid-liquid surface energy,  $\gamma_{sl}$ .

A common method to measure these quantities is the Wilhelmy Plate experiment; a thin substrate blade coated in the solid of interest is immersed in a liquid and then partially withdrawn. In addition to buoyancy, the force acting on the blade is due to the product of the surface tension of the liquid,  $\gamma_L$ , and the blade perimeter  $p$ . By using pairs of characterised liquids, simultaneous equations can be formed which may be solved for the solid's polar and dispersive surface energy components;  $\gamma_{sp}$  and  $\gamma_{sd}$ . By measuring the surface properties of energetic crystals and binders, the TWAs of potential PBX compositions can be calculated; an example of this approach is given by Rivera and Matuszak [5].

The TWA is often much smaller than the measured work of adhesion (MWA), which is the measured energy required to create new surface in a macroscopic experiment; such as a peel test or a



tensile butt-joint [6]; dissipative mechanisms such as viscoelastic loss and plastic deformation account for the differences.

Atomic force microscope (AFM) experiments to measure the pull-off force required to remove a calibrated functionalised tip [7] from a surface represent an intermediate class of adhesion experiment, where the deformations are deliberately kept elastic. A geometry of particular interest is an infinite half-plane (substrate) in contact with a sphere of known radius of curvature (spherical cap functionalised AFM probe). The measured pull-off force is the tensile force required to overcome the attractive surface interactions when pulling the sphere off the surface (debonding).

In the current study we present surface energy measurements of glass and the polymer KEL-F800 measured using the Wilhelmy Plate technique, which we combine to calculate the Thermodynamic Work of Adhesion. We also present data from AFM pull-off experiments conducted on the same materials and show that the TWA from the Wilhelmy Plate experiments can be used to predict the pull-off forces measured. The results validate the self-consistency of both types of experiment and give confidence when experimentally measured properties and quantities are incorporated into microstructurally resolved computational models of the deformation and fracture of composites [8].

## 2. Wilhelmy Plate

The technique used in the present study has its basis in the description by Rosano *et al.* [9]. It is regarded by Krishnan *et al.* [10] as being the most robust technique of those commonly available. We have previously reported its use in [6].

Standard glass microscope slides (26×1×76 mm) were used either bare (following cleaning in heated 70% conc. nitric acid and washing in ultra-pure water) or coated with KEL-F800 by dipping them into a binder solvent solution (10:1 methyl-ethyl-ketone : KEL-F800 granules). Dipping was performed at a rate of 2 mm min<sup>-1</sup> using an Instron machine.

Slides were hung from a mechanical microbalance (model: Mettler H5, single-pan, analytical balance) instead of the normal sample-pan. Reference liquids were raised up in glass troughs to the coated slides using a small laboratory jack. Depths of immersion were determined using a travelling microscope to measure the distance between the plane of the liquid-surface interface and the bottom of the immersed slides. The apparent increase/loss in weight due to the combined effects of interfacial tension and buoyancy were measured directly with the micro-balance previously tared to the weight of the coated slides. Measurements were taken both on immersion and removal, which correspond to both advancing and receding contact angle data, but only the advancing data are utilised here. Three repetitions were performed per sample type using fresh samples each time.

Three reference liquids were used: water (H<sub>2</sub>O), glycerol (C<sub>3</sub>H<sub>5</sub>(OH)<sub>3</sub>) and methylene iodide (CH<sub>2</sub>I<sub>2</sub>). Slides were only used once before being disposed of. Total immersion depths did not exceed 15 mm due to buoyancy forces exceeding the range of the microbalance. The regression fit to the force at zero advancing depth represents that force due only to the surface tension acting on the coated glass slides. The work of adhesion  $W_a$  between a liquid of surface tension  $\gamma_L$  which forms a perimeter  $p$  of contact angle  $\theta$  against the binder is related to the measured force  $f$  by:

$$W_a = \gamma_L + f/p = \gamma_L + \gamma_L \cos\theta, \quad (1)$$

Furthermore, in the analysis due to Kaelble [11] the interactions of a non-fully-wetting liquid on a solid surface can be described by:

$$W_a = 2\sqrt{(\gamma_L^d \gamma_S^d)} + 2\sqrt{(\gamma_L^p \gamma_S^p)}, \quad (2)$$

where the subscripts  $L$  and  $S$  denote properties of the liquid and solid respectively. Thus in equation (1) we have description of the work of adhesion in terms of measurable quantities, and in equation (2) a theoretical description from which we can calculate the unknown quantities of interest.

Equation (2) contains two unknowns: those of the polar and dispersive components of the binder's surface energy. When two liquids are considered, a set of simultaneous equations are created, which can be solved for the two unknowns. The use of three reference liquids allows for three pairs of simultaneous equations to be formed, *i.e.* AB, AC and BC. Each pair can be solved to give values for  $\gamma_p$  and  $\gamma_d$  for the solid. The results from the advancing measurements determined by solving these pairs of equations are given in table 1, along with the average  $\gamma_s$  values.

**Table 1.** Advancing immersion results for naked glass and KEL-F800.

Liquid pair	Glass			KEL-F800		
	$\gamma_s / \text{mJ m}^{-2}$	$\gamma_s^p / \text{mJ m}^{-2}$	$\gamma_s^d / \text{mJ m}^{-2}$	$\gamma_s / \text{mJ m}^{-2}$	$\gamma_s^p / \text{mJ m}^{-2}$	$\gamma_s^d / \text{mJ m}^{-2}$
H <sub>2</sub> O C <sub>3</sub> H <sub>5</sub> (OH) <sub>3</sub>	69.9 ± 0.6	68.7 ± 0.6	1.2 ± 0.1	29.5 ± 1.3	19.1 ± 1.1	10.4 ± 0.6
H <sub>2</sub> O CH <sub>2</sub> I <sub>2</sub>	56.7 ± 0.4	40.7 ± 0.4	16.0 ± 0.2	29.5 ± 1.0	22.4 ± 0.9	7.2 ± 0.4
C <sub>3</sub> H <sub>5</sub> (OH) <sub>3</sub> CH <sub>2</sub> I <sub>2</sub>	38.3 ± 0.9	18.4 ± 0.9	19.8 ± 0.2	33.0 ± 2.4	26.3 ± 0.9	6.7 ± 0.5
Mean value	<b>54.9 ± 0.4</b>	<b>42.6 ± 0.4</b>	<b>12.3 ± 0.1</b>	<b>30.6 ± 1.0</b>	<b>22.6 ± 0.9</b>	<b>8.1 ± 0.3</b>

As expected [11], the more polar reference liquids emphasise the polar character of the solids, and the more non-polar liquids emphasise the non-polar character of the solids. It is important to use reference liquids of both types to avoid biasing the mean calculated value of the solid surface energy. The KEL-F800 results agree favourably with those of Rivera and Matuszak [5] ( $\gamma_s = 32 \text{ mJ m}^{-2}$ ), and the glass results with those of Tsutsumi and Abe [12] ( $\gamma_s = 55 \text{ mJ m}^{-2}$ ). Using equation (2) again with the data in the above table 1, we arrive at a thermodynamic work of adhesion between glass and KEL-F800 of  $82 \pm 1 \text{ mJ m}^{-2}$ .

### 3. AFM Pull-off

KEL-F800 functionalised AFM probes are fabricated by attaching KEL-F800 droplets (spherical caps) to tip-less cantilevers on silicon AFM probes (model: NSC12 from MikroMasch). Each probe has three cantilevers with lengths 90, 110 and 130  $\mu\text{m}$ , which have been calibrated by the manufacturer to determine the spring constants using the method of Sader *et al.* [13]. Positioning of the droplets is performed using a micro-manipulator (model Narishige MMN-1) under an optical microscope. Figure 1 is an ESEM image of a functionalised tip showing the spherical cap of KEL-F800 on the end of a silicon cantilever. Using this approach, there is no excess of binder material present on the cantilever.

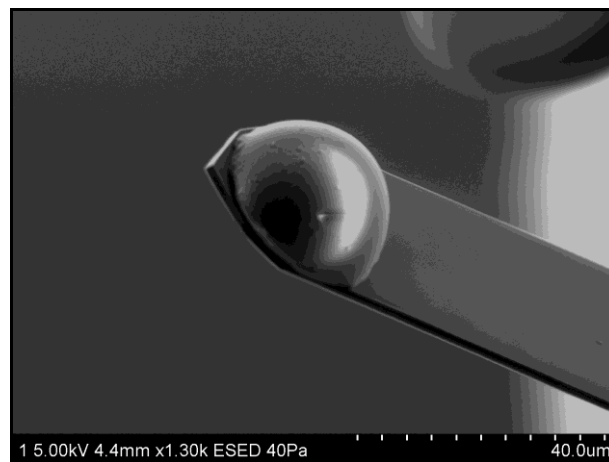


**Figure 1.** ESEM image of a KEL-F800 functionalised AFM probe.

Functionalised tips are AFM imaged with a standard probe to determine their radii of curvature. The  $x, y, z$  position data are fitted to a sphere in a least-squares-best-fit sense, typical RMS residuals over the fit are of order 100 nm, or 1% of the droplet radius of curvature.

The functionalised tips are installed into the AFM (model: Veeco diEnviroScope) along with the cleaned glass substrates (same process as for the Wilhelmy plate experiments) and the AFM is purged with dry nitrogen gas to remove ambient humidity. The functionalised tip is brought into contact with the glass substrate and loaded in compression to the target level of applied load, which is deliberately kept well below the level that would cause plastic deformation. The tip is then unloaded, and following null applied load being reached, the interface goes into tension, held together by adhesive interaction. At some point the applied tensile force becomes equal to, and then greater than, the adhesive force and the bond breaks, causing the cantilever to rebound sharply upwards. The force at this critical point is the measured pull-off force,  $P_c$ . In the JKR (Johnson-Kendall-Robinson) description of this geometry [14],  $P_c$  is given by

$$P_c = 3\pi R \left( \frac{W_a}{2} \right), \quad (3)$$

where  $R$  is the radius of curvature. The  $W_a$  term is the same thermodynamic work of adhesion that was determined in the Wilhelmy Plate experiments.

Figure 2 shows, for droplets of two different sizes, the expected result that the pull-off force is independent of the applied force (provided there is no plastic deformation). Figure 3 shows the expected linear dependence of pull-off force upon droplet radius of curvature. In each case, we plot the expected values of pull-off force based upon the measured Wilhelmy Plate data of section 2. Each AFM pull-off force data point represents the average value of either 9 or 25 individual measurements and the error bars give the standard deviations. A linear fit to the AFM pull-off data as a function of droplet radius (shown in figure 3) gives a value of  $W_a = 81 \pm 4 \text{ mJ m}^{-2}$ , and is in excellent agreement with the value of  $82 \pm 1 \text{ mJ m}^{-2}$  from the Wilhelmy Plate experiments.

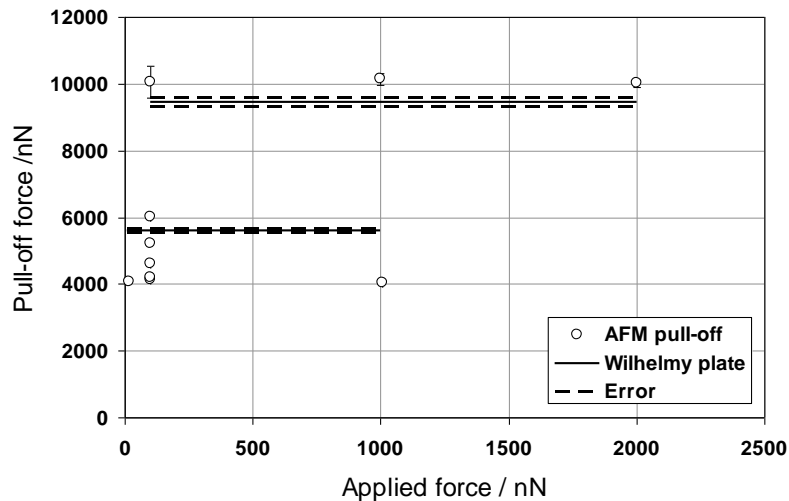


**Figure 2.** Pull-off force as a function of applied force for a droplet with a radius of curvature of: top dataset 24.5  $\mu\text{m}$ , bottom dataset 14.5  $\mu\text{m}$ . As expected there is no dependence on applied force. Data points were measured in the AFM, solid lines give the values expected from the JKR theory using Wilhelmy Plate surface energy data. The 14.5  $\mu\text{m}$  droplet data points were taken with the same AFM probe but a number of different substrates, the three data points at approximately 4000 nN pull-off force were all taken with the same substrate.

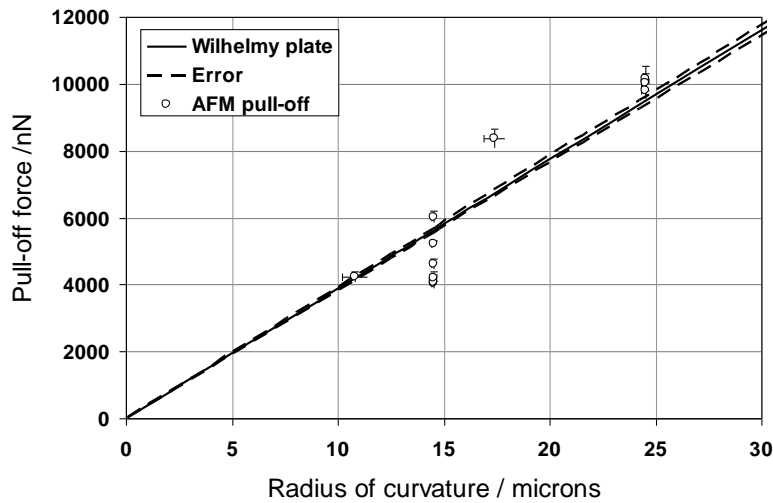


**Figure 3.** Pull-off force as a function of droplet radius of curvature. Data points were measured in the AFM, while the solid line gives the expected pull-off force variation based upon JKR theory using Wilhelmy Plate surface energy data. The points at 14.5  $\mu\text{m}$  radius were taken with the same AFM probe but a number of different substrates.

It is often useful to have a stress based failure criterion. Another prediction of the JKR model [14] is that the critical radius of circular contact area,  $a_c$ , at pull-off is given by:

$$a_c = \left( \frac{9\pi\gamma R^2}{4E^*} \right)^{1/3}, \quad (4)$$

where the effective modulus  $E^*$  is given by:

$$E^* = \left( \frac{1-\nu_1^2}{E_1} + \frac{1-\nu_2^2}{E_2} \right)^{-1}, \quad (5)$$

and where  $E_1$  &  $E_2$  and  $\nu_1$  &  $\nu_2$  are the corresponding values for the elastic moduli and Poisson's ratio of the interacting materials. As might be expected, large particles debond at lower stresses than smaller ones; in this particular geometry  $\sigma_F \propto R^{(-1/3)}$ , whereas for a rigid spherical inclusion embedded in a soft matrix  $\sigma_F \propto R^{(-1/2)}$  [15]. This last point is important because real PBXs deliberately make use of range of filler particle sizes.

#### 4. Conclusions

A series of experiments have been performed which demonstrate that the Thermodynamic Work of Adhesion calculated from the free surface energies measured in Wilhelmy Plate experiments can be used to predict the pull-off forces measured in AFM experiments using calibrated functionalised tips. The two approaches are experimentally very different; the excellent agreement between the two datasets demonstrates their reliability. An advantage of the AFM approach to measuring adhesive parameters is that it readily lends itself to investigating the role of temperature, humidity, strain-rate, and surface roughness in a controlled manner. These techniques can provide the data required to develop and validate microstructurally resolved computational micro-models of the deformation and fracture of PBXs.

### Acknowledgements

The authors thank AWE plc for sponsoring this research and supplying materials.

### References

- [1] Palmer S J P, Field J E and Huntley J M 1993 *P. Roy. Soc. Lond. A* **440** 399-414
- [2] Rae P J, Goldrein H T, Palmer S J P, Field J E and Lewis A L 2000 *11th Int. Detonation Symp. (Snowmass, CO, 31 August - 4 September 1998) (Portland, OR: Office of Naval Research, ONR 33300-5)* pp 66-75
- [3] Rae P J, Palmer S J P, Goldrein H T, Field J E and Lewis A L 2002 *P. Roy. Soc. Lond. A* **458**, 2227-42
- [4] Williamson D M, Palmer S J P, Proud W G and Govier R 2009 *AIP Conf. Proc.* **1195** pp 494-7
- [5] Rivera T and Matuszak M L 1982 *J. Colloid Interface Sci.* **93** 105-8
- [6] Williamson D M, Palmer S J P, Proud W G and Govier R 2009 *AIP Conf. Proc.* **1195** pp 478-81
- [7] Lin A Y M, Brunner R, Chen P Y, Talke F E and Meyers M A 2009 *Acta Mater.* **57** 4178-85.
- [8] Tarleton E, Charalambides M N and Leppard C 2012 *Comp. Mater. Sci.* **64** 183-6
- [9] Rosano H L, Gerbacia W, Feinstein M E and Swaine J W 1971 *J. Colloid Interface Sci.* **36** 298-307
- [10] Krishnan A, Liu Y H, Cha P, Woodward R, Allara D and Vogler E A 2005 *Colloid. Surface. B* **43** 95-8
- [11] Kaelble D H 1970 *J. Adhesion* **2** 66-81
- [12] Tsutsumi K and Abe Y 1989 *Colloid Polym. Sci.* **267** 637-642
- [13] Sader J E, Chon J W M and Mulvaney P 1999 *Rev. Sci. Instrum.* **70** 3967-69
- [14] Johnson K L 1985 *Contact Mechanics* (Cambridge, UK: Cambridge University Press)
- [15] Gent A N 1980 *J. Mat. Sci.* **15** 2884-8.